Journal of Southeast University (English Edition) Vol. 39, No. 4, pp. 333 - 339 Dec. 2023 ISSN 1003—7985

# Analysis of wind vibration response of suspended derrick under downburst

Lin Yuxuan Xu Zidong Wang Hao Liu Yaodong Zhang Han Zhao Kaiyong

(Key Laboratory of Concrete and Prestressed Concrete Structure of Ministry of Education, Southeast University, Nanjing 211189, China)

**Abstract:** The vibration response of a suspended derrick was analyzed using the finite element method to accurately estimate its safety performance in a transmission structure under a downburst. Based on the deterministic-random hybrid model, the entire process wind speed of the moving downburst is simulated by a modified stochastic wave-based spectral representation method. Meanwhile, the vibration response of the suspended derrick under a downburst was obtained. The results show that the suspended derrick swings considerably under a moving downburst, and the main structure bends with a displacement amplitude of approximately 1.388 m. Moreover, the maximum tension experienced by the outer tie line and supporting rope are 45.11 and 47.06 kN, respectively. The maximum displacement and tensile force values are observed when the center of the downburst is approximately 1 100 m away from the suspended derrick. This indicates that the suspended derrick is prone to produce a large wind vibration response under the downburst, which will adversely affect the construction safety of the transmission tower. Therefore, performing relevant reinforcement and vibration reduction control measures is essential.

**Key words:** moving downburst; suspended derrick; deterministic-random hybrid model; finite element simulation

**DOI:** 10.3969/j.issn.1003 - 7985.2023.04.002

Derrick is an important lifting equipment for transmission tower setup and is mainly divided into two categories: seat ground and suspended derricks[1]. The suspended derrick has been widely used in mountainous areas and other complex construction sites because of its advantages, such as strong adaptability and ease of transport. However, the suspended derrick is only restrained by the tie lines at both ends, making it a typical wind-sensitive structure with a large slenderness ratio, low damping, and poor wind stability[2]. With the deterioration of the global climate in recent years, an increase in exceptional wind hazards like typhoons, tornados, and downbursts will pose a severe threat to the suspended derrick. As one of the typical exceptional wind disasters, a downburst is characterized by strong suddenness, high wind speed, and great destructive power[3-4]. Therefore, analyzing the vibration response of a suspended derrick under a downburst is critical.

To this end, some research has been conducted on the wind-induced vibration response characteristics of transmission tower structures. For example, Hua et al.[5] estimated the effect of different turbulence integration scales on the wind vibration response of transmission towers. They proposed theoretical values for the wind-induced vibration coefficients by conducting wind tunnel tests using the air-elastic model. Wang et al.[6] proposed a frequency domain theoretical analysis method for estimating the nonstationary fluctuating response of transmission towers under downbursts based on the stochastic vibration theory. Zhao et al.[7] studied the wind-induced vibration response law of transmission towers with different heights and summarized the wind effect on various types of transmission towers under downbursts. Hamada et al.[8] determined the maximum wind speed that a derrick can withstand safely by analyzing the coupling system with a seat-ground double rocker derrick and tower. Deng et al.[9] clarified several factors affecting the wind-resistant performance of suspended derricks under working and non-working conditions. Huang et al.[10] investigated the vibration response characteristics of a derrick-tower coupled system and fatigue damage law of component vortex vibration by performing wind tunnel tests and finite element analysis. In April 2019, our research team recorded a downburst attack using the anemometer of the Sutong Bridge and analyzed the vibration response of the cable under this downburst[11]. However, most of the existing research has only focused on transmission towers and was limited to investigating the effect of conventional wind environment conditions on towers. Additionally, less attention has been devoted to studying wind effects on a suspended derrick under a downburst.

In this paper, a suspended derrick, which is established on a transmission structure under construction in the Yilu-Xuwei 500 kV line, is taken as the background. A finite element model of the suspended derrick is established using the ANSYS software. Additionally,

**Received** 2023-08-08, **Revised** 2023-09-10.

**Biographies:** Lin Yuxuan (2000—), male, Ph. D. candidate; Wang Hao (corresponding author), male, doctor, professor, wanghao1980@seu.edu.cn.

**Foundation items:** The National Natural Science Foundation of China (No. 52338011, 51978155, 52208481), China Postdoctoral Science Foundation (No. 2023M730581).

**Citation:** Lin Yuxuan, Xu Zidong, Wang Hao, et al. Analysis of wind vibration response of suspended derrick under downburst[J]. Journal of Southeast University (English Edition), 2023, 39(4): 333 - 339. DOI: 10.3969/j.issn.1003 - 7985.2023.04.002.

in order to clarify the dynamic characteristics of the structure, the modal analysis of the model is also conducted. Meanwhile, based on the deterministic-stochastic hybrid model, a moving downburst field is simulated using the harmonic superposition method. Finally, the vibration response of the suspended derrick under the downburst is calculated and analyzed. The findings of this study can provide a reference for addressing the wind resistance problem of transmission structures under construction.

## 1 Finite Element Model of Suspended Derrick

### 1.1 Model parameters

The geometric parameters of the finite element model used in this work are established according to the GNB28-55 type suspended derrick. The two ends of the suspended derrick are rectangular cross-sections with dimensions of 250 mm × 250 mm, and its central standard section has a dimension of 550 mm × 550 mm. The specific geometric parameters of the suspended derrick are shown in Fig. 1. Furthermore, the suspended derrick is mainly made of $\phi$50 mm × 3 mm and $\phi$32 mm × 3 mm round steel tubes. The connecting parts between each section are welded with ∠63 mm × 6 mm angle steel to form flange joints. The outer tie line and supporting rope are made of steel strands with a diameter of 15 mm. To calculate the vibration response of the suspended derrick under the downburst, the main structure and tie line are simulated using Beam188 and Link10 units, respectively. Additionally, Q345 steel is chosen as the material for derrick component and has a modulus of elasticity of 210 GPa and a density of 7.85 g/cm$^3$. Fig. 2 shows the finite element model of the suspended derrick. According to the site tower formation (see Fig. 3), the bottom of the suspended derrick is bound to the transmission tower using the supporting rope, while its top section is connected to the ground anchor via the outer tie line. Therefore, the anchorage end of the outer tie line and supporting rope in this analysis is fully restrained. The other end is articulated with the top/bottom corners of the derrick. Additionally, a 20 kN pre-tensioning force is set for each line separately by applying the initial strain.

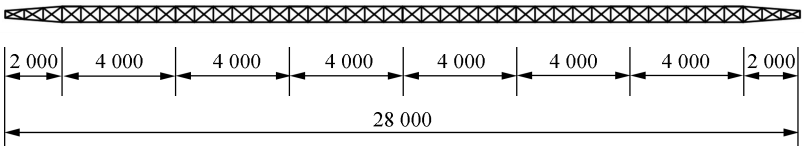


**Fig. 1** Geometry of the GNB28-55 suspended derrick (unit: mm)

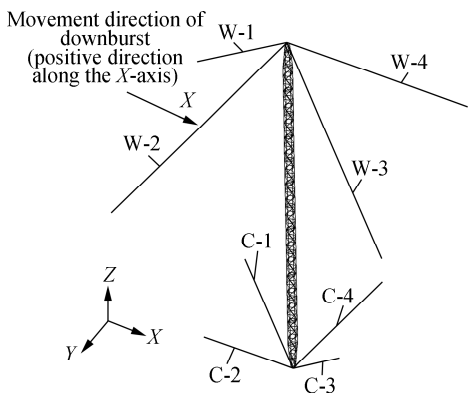


**Fig. 2** FEM of the suspended derrick

**Fig. 3** Construction site of the suspended derrick

### 1.2 Modal analysis

In the analysis, the Block Lancoz method is used to obtain the first 20 orders of modes of the suspended derrick. The results are verified using the ABAQUS software. A part of the modal vibration patterns is shown in Fig. 4. Table 1 presents the first five orders of modal frequencies from two software used to validate the finite element model.

Fig. 4 and Table 1 show that the vibration shapes obtained using the two software calculations are the same, and the frequency error is small. Therefore, the model has a certain degree of rationality. The first five orders of vibration modes include orthogonal side swing, horizontal torsion, and first-order bending. The structure has a low natural frequency of approximately 0.113 Hz. Since the outer tie line and supporting rope are articulated with the derrick through snap, their constraints on the structure are limited. Therefore, the suspended derrick is very prone to lateral swaying in the air. Additionally, the higher-order

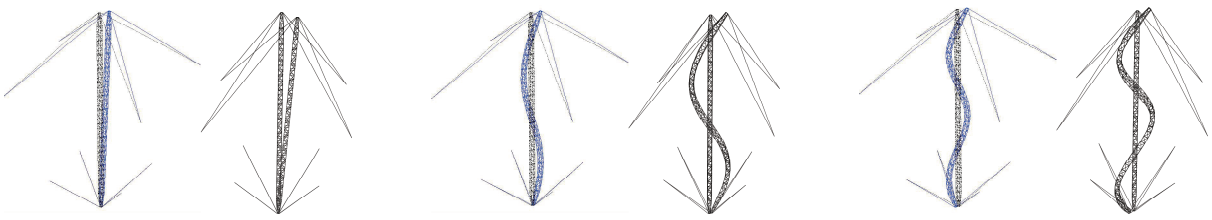


**Fig. 4** Partial vibration modes of the suspended derrick. (a) First-order modes; (b) Sixth-order modes; (c) Ninth-order modes

**Table 1** First five orders of intrinsic frequency and vibration pattern of the suspended derrick

| Orders | Frequency of ANSYS/ Hz | Frequency of ABAQUS/ Hz | Relative error/ % | Vibration mode |
|---|---|---|---|---|
| 1 | 0.113 | 0.110 | 2.67 | Transversal swing |
| 2 | 0.113 | 0.110 | 2.67 | Vertical swing |
| 3 | 0.906 | 0.900 | 0.66 | Horizontal torsion |
| 4 | 2.440 | 2.413 | 1.22 | Transversal first-order bending |
| 5 | 2.440 | 2.413 | 1.22 | Vertical first-order bending |
| 6 | 7.891 | 7.833 | 0.67 | Transversal second-order bending |
| 7 | 7.891 | 7.833 | 0.67 | Vertical second-order bending |
| 8 | 13.177 | 13.025 | 1.13 | Horizontal second-order torsion |
| 9 | 16.092 | 16.028 | 0.47 | Transversal third-order bending |
| 10 | 16.092 | 16.028 | 0.47 | Vertical third-order bending |

Note: Transversal and vertical are the direction of the angular bisector of the angle of the outer tie line.

modes of suspended derrick are dominated by the bending vibration pattern because of the existence of pre-pressure from the tension line.

## 2 Wind Field of Moving Downburst

The wind field of the downburst is random, nonstationary, and hard to obtain using traditional methods, such as measured data and wind tunnel tests[12]. Therefore, herein, the method used for estimating wind field is based on a numerical simulation approach that combines a deterministic-stochastic hybrid model[13] with a modified stochastic wave-based spectral representation method[14] to simulate the wind speed time history course of a moving downburst. The wind speed $U(z, t)$ at any location in the wind field can be decomposed into time-varying mean wind speed $\bar{U}(z, t)$ and fluctuating wind speed $u(z, t)$ because the moving downburst has vertical and radial wind profiles.

### 2.1 Time-varying mean wind field model

A time-varying mean wind field can be assumed, where the mean wind speeds at different heights in a downburst reach their maximum values simultaneously at a certain moment. To this end, the deterministic-stochastic hybrid model proposed by Chen and Letchford[13] is used to generate a downburst averaged wind speed time history. The time-varying average wind speed $\bar{U}(z, t)$ can be expressed as the product of the vertical wind speed profile and the time function:

$$\bar{U}(z, t) = V(z) f(t) \tag{1}$$

where $V(z)$ denotes the maximum mean wind speed profile and $f(t)$ denotes the function of time. Few analytical models like the O&B[15], Vicroy[16], and Wood models[17] can find $V(z)$. In this work, the Vicroy empirical analytical model is selected because its wind velocity profile is closer to the existing measured results:

$$V(z) = 1.22 \times (\mathrm{e}^{0.15 z/z_{\max}} - \mathrm{e}^{3.217 5 z/z_{\max}}) U_{\max} \tag{2}$$

where $Z_{\max}$ is the height corresponding to the maximum horizontal wind speed of the downburst; $U_{\max}$ denotes the maximum horizontal wind speed in the vertical profile.

The time function $f(t)$ is defined as the ratio of the mean wind speed $|V_c(t)|$ to the maximum mean value $\max|V_c(t)|$ at any instant in time, where $V_c(t)$ can be expressed as the vector sum of the radial wind speed $V_r(t)$ and the velocity of the center of the downburst $V_t$. The radial wind speed of the downburst is modeled using the radial wind speed profile model based on time decay proposed by Holmes et al.[18] with the following expression:

$$V_r(t) = \begin{cases} V_{r,\max} \mathrm{e}^{-t/T} \left( \dfrac{r}{r_{\max}} \right) & 0 \ll r < r_{\max} \\ V_{r,\max} \mathrm{e}^{-t/T} \mathrm{e}^{-[(r - r_{\max})/R_r]^2} & r \gg r_{\max} \end{cases} \tag{3}$$

where $r$ denotes the distance of the derrick point from the center of the downburst at moment $t$; $V_{r,\max}$ represents the maximum radial jet velocity; $r_{\max}$ denotes the radial distance to reach maximum radial jet velocity; $R_r$ denotes the characteristic radius, and $T$ denotes the duration of the downburst.

This paper uses the wind speed data measured at Andersen Air Force Base published by Fujita[19]. It is assumed that the downburst flow passes through the suspended derrick along the $X$-axis, and the movement path is shown in Fig. 5. The center of the downburst at the initial moment is 3 500 m away from the suspended derrick, and

the relevant parameters are $V_t = 8$ m/s, $V_{r,\max} = 47$ m/s, $r_{\max} = 1\,000$ m, $R_r = 700$ m, and $T = 1\,024$ s. The time-varying mean wind speed at any height of the derrick can be obtained by calculating the vertical wind profile of the downdraft wind field (see Fig. 6) according to Eqs. (1)-(3).

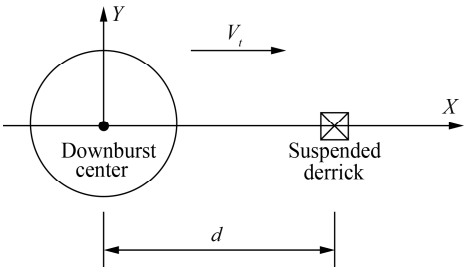


**Fig. 5** Downburst movement path

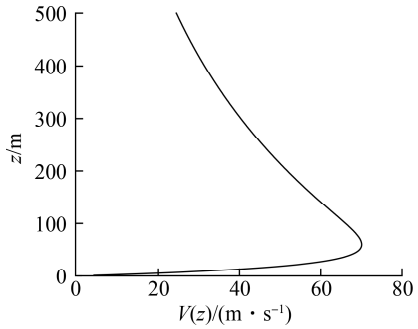


**Fig. 6** Downburst vertical wind profile

## 2.2 Fluctuating wind field model

To simulate the strong nonstationarity of fluctuating wind of the downburst, it can be expressed as the product of a time-varying modulation function and a stationary Gaussian stochastic process with a given power spectrum[20]:

$$u(z,t) = \alpha(z,t)\,k(z,t) \tag{4}$$

where $\alpha(z,t)$ denotes the modulation function that takes the value of 0.25 times the time-varying mean wind speed according to Chen and Letchford[13]; $k(z,t)$ denotes the stationary Gaussian stochastic processes that follow the standard normal distribution. $k(z,t)$ can be generated through simulation using the harmonic superposition method, and its self-power spectral density function uses the normalized Kaimal spectrum[14]:

$$S_u(n) = u_*^2 \frac{200f}{n(1+50f)^{5/3}} \tag{5}$$

where $u_*$ denotes the friction velocity; $f = nz/v_z$ denotes the Monin coordinate; $n$ denotes the natural frequency; $v_z$ denotes the average wind speed at height $z$. The correlation function proposed by Davenport is used in this analysis to consider the spatial correlation between different simulation points (SP). The fluctuating wind speeds at nine SPs from different heights of suspended derrick (see Fig. 7) are simulated with a sampling frequency of approximately 4 Hz. Fig. 8 shows the wind speed time history of the entire process downburst at SP5.

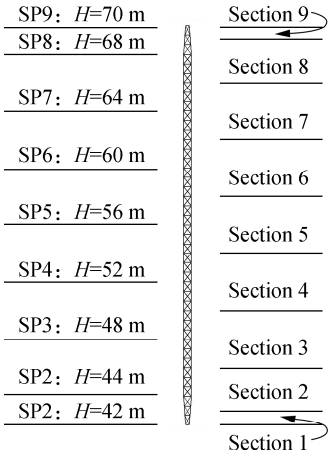


**Fig. 7** Simulation point heights in the derrick

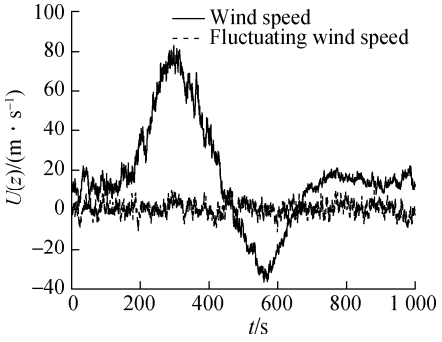


**Fig. 8** Wind speed of SP5

The validity of the simulated wind speed is examined through the power spectral density and correlation function. As shown in Figs. 9 and 10, the power spectrum of the simulated wind field is consistent with the Kaimal spectrum. Additionally, the theoretical value of the correlation function overlaps well with the target value. These results show that the simulated wind speed of the downburst is valid and can be used for the dynamic time-range analysis of the structure.

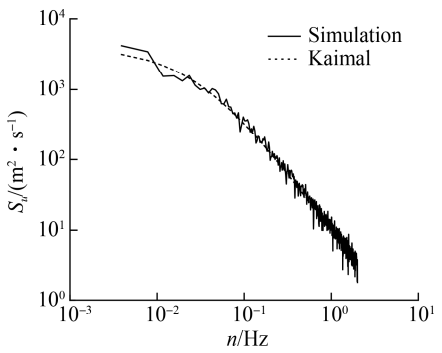


**Fig. 9** Comparison between simulated and Kaimal spectra

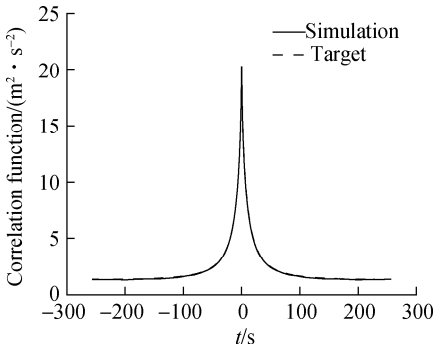


**Fig. 10** Comparison between simulated and target correlation functions

## 3 Wind Vibration Response of Suspended Derrick under Moving Downburst

### 3.1 Wind load modeling for moving downburst

According to the simulated wind speed of the moving downburst, the along- and cross-wind loads can be calculated based on the quasistationary assumption. The specific expressions are as follows:

$$F_u(t) = 0.5\rho[\bar{U}(z,t) + u_u(z,t)]^2 B(z) C_u(z) \quad (6)$$

$$F_w(t) = 0.5\rho[u_w(z,t)]^2 B(z) C_w(z) \quad (7)$$

where $\rho$ denotes the air density, which takes the value of 1.29 kg/m$^3$; $\bar{U}(z,t)$ denotes the mean wind speed, and $u_u(z,t)$ and $u_w(z,t)$ denote the along- and cross-fluctuating wind speeds, respectively. $B(z)$ denotes the projected area of the section in the vertical wind direction. Here, $C_i(z)$ ($i$ = u, w) denotes the shape factor of wind load and is set at 1.95 according to the load code for the overhead transmission line design (DL/T 5551—2018). Subsequently, the obtained wind loads are applied to nine simulation points, and the entire process dynamic response of the suspended derrick is calculated using the transient analysis method. The damping of the suspended derrick is determined using the Rayleigh damping formula and is set as 0.004 and 0.038 for mass and stiffness damping, respectively.

### 3.2 Vibration response analysis of the main structure

Based on the calculation result of vibration response, the time history of downwind displacements at the top (SP9), middle (SP5), and bottom (SP1) of the suspended derrick during the downburst attack is shown in Fig. 11. As mentioned earlier, the moving downburst reaches the location of the suspended derrick at approximately $t$ = 437.5 s and continues to move away from the transmission tower construction site. Therefore, Fig. 11 shows that when the downburst moves toward the suspended derrick, its downwind displacement first increases and then decreases. Notably, the maximum displacement occurs around $t$ = 300 s (the center of the downburst is 1 100 m away from the suspended derrick). Comparing the displacement amplitude of the suspended derrick at each simulation point under downburst, the value of the middle section is the largest, which is 1.388 m. Additionally, the bottom and top values are 0.028 and 0.210 m, which are much smaller than the middle section. Therefore, the deformation of the derrick is mainly bending when the wind speed of the downburst is maximum. Additionally, a large swing occurs, which is consistent with the dynamic characteristics analysis in Section 1.

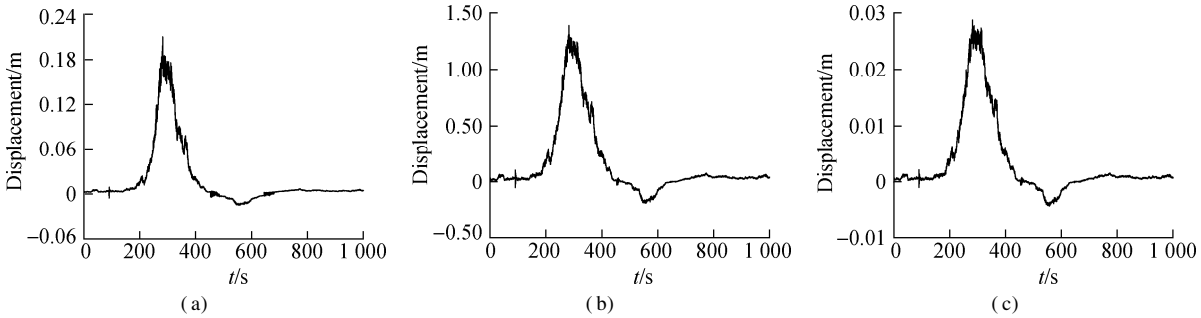


**Fig. 11** Time course of along wind displacement ($X$-direction) at some nodes of the suspended derrick. (a) Top section; (b) Middle section; (c) Bottom section

After the center of the moving downburst passes through the suspended derrick, the direction of the wind field changes from the incoming flow to the outgoing flow. Therefore, the displacement response of the derrick is negative. The absolute value of the displacement also increases and then decreases, reaching a second peak at approximately $t$ = 550 s. However, the displacement amplitude caused by the outgoing flow is much smaller than that of the incoming flow. The value is approximately 7% to 15% of the first peak. After the downburst through the suspended derrick, the wind speed acting on the structure is relatively small compared to the incoming flow because the radial wind and moving wind speeds are in opposite directions. This is mainly because the response of the structure is much smaller than that of the incoming flow acting. Furthermore, the PSD of response is analyzed to investigate the dominant frequency of the suspended derrick under downburst. The results show that

the dominant frequency is 1.032 Hz, which is close to the third-order mode of the suspended derrick. Therefore, it is necessary to focus on the structural response before the center of the downburst reaches the suspended derrick.

### 3.3 Vibration response analysis of tension lines

According to the number of the tension lines in Fig. 2, the vibration response of the outer tie lines W-1 and W-4 and the supporting ropes C-1 and C-4 are selected for analysis, and their tension time history curves are shown in Figs. 12 and 13.

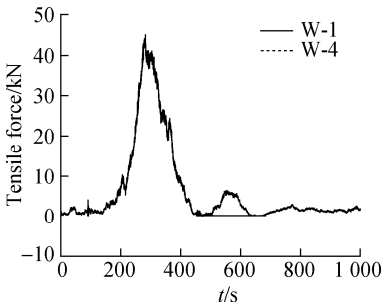


**Fig. 12** The tensile force of outer tie lines

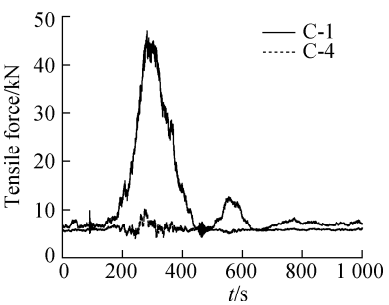


**Fig. 13** The tensile force of inner ropes

As shown in Figs. 12 and 13, when the center of the downburst is close to the suspended derrick, the outer tie lines W-1 and W-2 and the inner ropes C-1 and C-2 are pulled taut because of the horizontal displacement of the top and bottom of the derrick. Additionally, their tensile force increases with increasing displacement. The maximum tensile forces experienced by the outer tie lines and supporting ropes are 45.11 and 47.06 kN, respectively. Here, the outer tie lines W-3 and W-4 are in a slack state, and their tension is 0. Meanwhile, the supporting ropes C-3 and C-4 only need to bear the self-weight of the derrick, and their tension does not change considerably with wind speed or derrick displacement.

When the horizontal displacement direction of the derrick changes from positive to negative, the states of the outer tie line and supporting rope also vary. The outer tie lines W-3 and W-4 are pulled taut, and the tension gradually increases from 0 to 6.43 kN and then gradually decreases until the displacement is positive, at which point its tension becomes zero again. The tension of the supporting ropes C-3 and C-4 gradually increases from 5.87 kN to a maximum value of 12.71 kN. Consequently, when a downburst hits the derrick, the ground anchor of the outer tie line, the connection joint at the two ends of the derrick, and the main rod in the transmission towers connected to the supporting rope need to be reinforced to ensure that they can withstand more than 50 kN of tension. Ensuring that the steel strand used for making the outer tie line and supporting rope has sufficiently high tensile strength is necessary to confirm the safety of equipment and personnel at the construction site when encountered by a downburst.

## 4 Conclusions

1) The three types of the first five-order modal vibration patterns of the suspended derrick are lateral sway, horizontal torsion, and first-order bending. The natural frequency of the structure is only 0.113 Hz, indicating that the suspended derrick is a wind load-sensitive structure.

2) When the moving downburst is 1 100 m away from the suspended derrick, it swings considerably and exhibits obvious bending deformation, reaching a displacement amplitude of 1.388 m. The effect of the downburst is substantially reduced when the wind center moves away from the structure. Further, the displacement amplitude reduces to 7%-15% of the first peak.

3) The pulling forces of the outer tie line and supporting rope on the incoming flow side increase and then decrease with wind speed. The maximum values of pulling forces observed for the outer tie line and supporting rope are 45.11 and 47.06 kN, respectively. Therefore, the suspended derrick is prone to produce a large wind vibration response under a downburst, adversely affecting the construction safety of the transmission tower.

## References

[1] Huang M F, Wei X R, Ye H K, et al. Wind-induced response of crane structure with double flat arms for long-span transmission towers[J]. *Journal of Zhejiang University (Engineering Science)*, 2021, **55**(7): 1351 − 1360. (in Chinese)

[2] Zhang Z Q, Li H N, Li S F, et al. Dynamic response analysis of transmission tower under wind-sand load induce[J]. *Journal of Southeast University (Natural Science Edition)*, 2018, **48**(3): 506 − 511. DOI: 10.3969 / j.issn.1001-0505.2018.03.019. (in Chinese)

[3] Ji B F, Zhao J X, Jiang F, et al. Variation characteristics of wind pressure on heliostat under impact of downburst strong wind[J]. *Journal of Southeast University (Natural Science Edition)*, 2021, **51**(5): 790 − 796. DOI: 10.3969/j.issn.1001-0505.2021.05.009. (in Chinese)

[4] Wang H, Xu Z D, Tao T Y, et al. Analysis on joint distribution of wind speed and direction on Sutong Bridge based on measured data from 2008 to 2015[J]. *Journal of*

*Southeast University* (*Natural Science Edition*), 2016, **46** (4): 836 - 841. DOI: 10. 3969/ j. issn. 1001-0505. 2016. 04. 027. (in Chinese)

[5] Hua X G, Chen Z Q, Yang J B, et al. Turbulence integral scale corrections to aeroelastic wind tunnel experimental results with large scale model[J]. *Journal of Building Structures*, 2010, **31**(10): 55 - 61. DOI: 10. 14006/j. jzjgxb. 2010. 10. 008. (in Chinese)

[6] Wang D H, Wang G Q, Wang X, et al. Frequency domain method for dynamic responses of transmission tower under downburst[J/OL]. *Engineering Mechanics*. (2023-02-25) [2023-07-09]. http:// kns. cnki. net/ kcms/ detail/ 11. 2595. O3. 20230223. 1651. 012. html. (in Chinese)

[7] Zhao Y, Sun Q G, Song Z Y, et al. A dynamic responses and evaluation method of the downburst wind loads effect on a transmission tower[J]. *Journal of Vibration and Shock*, 2021, **40**(12): 179 - 188, 195. DOI: 10. 13465/j. cnki. jvs. 2021. 12. 022. (in Chinese)

[8] Hamada A, King J P C, El Damatty A A, et al. The response of a guyed transmission line system to boundary layer wind[J]. *Engineering Structures*, 2017, **139**: 135 - 152. DOI: 10. 1016/j. engstruct. 2017. 01. 047.

[9] Deng H Z, Xu H J, Ma X. Wind-vibration coefficient of guyed masts[J]. *Journal of Vibration and Shock*, 2016, **35**(22): 48 - 53. DOI: 10. 13465/j. cnki. jvs. 2016. 22. 008. (in Chinese)

[10] Huang S, Huang M F, Ye H K, et al. Dynamic wind induced vibration and fatigue damage analysis of heliostat structures[J]. *Engineering Mechanics*, 2017, **34**(12): 120 - 130. DOI: 10. 6052/j. issn. 1000-4750. 2016. 08. 0612. (in Chinese)

[11] Zhang H, Wang H, Xu Z D, et al. Monitoring-based analysis of wind-induced vibrations of ultra-long stay cables during an exceptional wind event[J]. *Journal of Wind Engineering and Industrial Aerodynamics*, 2022, **221**: 104883. DOI: 10. 1016/j. jweia. 2021. 104883.

[12] Lang T Y, Wang H, Jia H Z, et al. Vortex-induced vibration performance and wind pressure distribution of main girder of long-span suspension bridge affected by temporary facilities[J]. *Journal of Southeast University* (*Natural Science Edition*), 2022, **52**(5): 833 - 840. DOI: 10. 3969/ j. issn. 1001-0505. 2022. 05. 002. (in Chinese)

[13] Chen L Z, Letchford C W. A deterministic-stochastic hybrid model of downbursts and its impact on a cantilevered structure[J]. *Engineering Structures*, 2004, **26**(5): 619 - 629. DOI: 10. 1016/j. engstruct. 2003. 12. 009.

[14] Zhao K Y, Wang H, Xu Z D. Simulation of turbulent wind field in multi-spatial dimensions using a novel non-uniform FFT enhanced stochastic wave-based spectral representation method[J]. *Mechanical Systems and Signal Processing*, 2023, **200**: 110520. DOI: 10. 1016/j. ymssp. 2023. 110520.

[15] Oseguera R M, Bowles R L. A simple, analytic 3-dimensional downburst model based on boundary layer stagnation flow[J]. *NASA Technical Memorandum*, 1988, **7**: 1 - 17.

[16] Vicroy D D. A Simple, analytical, axisymmetric microburst model for downdraft estimation[J]. *NASA Technical Memorandum*, 1991, **5**: 1 - 11.

[17] Wood G S, Kwok K C S, Motteram N A, et al. Physical and numerical modelling of thunderstorm downbursts[J]. *Journal of Wind Engineering and Industrial Aerodynamics*, 2001, **89**(6): 535 - 552. DOI: 10. 1016/S0167-6105(00)00090-8.

[18] Holmes J D, Oliver S E. An empirical model of a downburst[J]. *Engineering Structures*, 2000, **22**(9): 1167 - 1172. DOI: 10. 1016/S0141-0296(99)00058-9.

[19] Fujita T T. The downburst: Mieroburst and macroburst: report of projects NIMROD and JAWS[R]. Chicago, IL, USA: University of Chicago, 1985.

[20] Li Y, Huang G Q, Cheng X, et al. The numerical simulation of moving downbursts and their induced wind load on high-rise buildings[J]. *Engineering Mechanics*, 2020, **37**(3): 176 - 187. (in Chinese)

# 下击暴流作用下悬浮抱杆的风振响应分析

林禹轩　徐梓栋　王　浩　刘耀东　张　寒　赵恺雍

(东南大学混凝土及预应力混凝土结构教育部重点实验室, 南京 211189)

**摘要**:为准确评估下击暴流作用下输电塔施工场地抱杆的安全性能,采用有限元方法分析了悬浮抱杆的风振响应特性. 基于确定性-随机混合模型,通过改进的随机波数谱方法模拟移动下击暴流的全过程风速,计算得到了悬浮抱杆在下击暴流作用下的风振响应. 结果表明:悬浮抱杆在移动下击暴流的作用下将发生大幅摆动,同时主体结构出现弯曲变形,其中抱杆中段的顺风向位移幅值可达 1. 388 m,外拉线拉力最大值为 45. 11 kN,承托绳的最大拉力为 47. 06 kN,悬浮抱杆主体结构的最大位移及拉线的最大拉力均在下击暴流中心距离悬浮抱杆 1 100 m 附近时出现. 可见,下击暴流作用下悬浮抱杆易产生较大的风振响应,将对输电塔的施工安全产生不利影响,有必要采取相关的加固与减振控制措施.

**关键词**:移动下击暴流;悬浮抱杆;确定性-随机混合模型;有限元模拟

**中图分类号**:TU351